Elastically coupled two-dimensional Brownian motors

Hiromichi Goko

Faculty of Economics, Kyoto University, Kyoto 606-8501, Japan

Akito Igarashi

Department of Applied Mathematics and Physics, Kyoto University, Kyoto 606-8501, Japan

Many workers have theoretically and numerically studied Brownian motors (ratchet models) as models for molecular motors for many years. Their studies have been mainly concerned about one-dimensional motion of a particle or coupled particles experiencing spatially asymmetric interaction force. In this paper, we introduce a coupled flashing ratchet model, that is, elastically coupled Brownian particles with their own easily advancing directions under the on-and-off (or occasional) influence of two-dimensional interaction force asymmetric in the easily advancing direction of each particle. The dynamics of the model is investigated by computer simulation and characteristic motion of the particles in the two-dimensional space is observed. Our model is also studied as that for molecular motors in muscle contraction and the simulation results are compared with those of *in vitro* biological experiments in motility assays of the molecular motors. We succeed in reproducing the experimental results qualitatively with our model.

I. INTRODUCTION

Brownian motors, especially "ratchet" models, have been widely studied by many workers recently [1–5]. Theoretically, the ratchet models are quite interesting as an application of stochastic processes to transport phenomena. Without any directed force, these models realize transport with mechanism completely different from those in standard directional motion. It is found that thermal noise, proper spatially asymmetric interaction force, and energy injection mechanism can produce the macroscopic motion of a particle toward a particular direction which depends on the asymmetric properties of the interaction force. The coupled "ratchet" models where particles interact mutually have been also studied recently from theoretical interest in the effects of mutual interaction among particles on transport phenomena. As an application of stochastic processes, some workers have been studying the dynamical properties of the coupled ratchet models [6]. Jülicher, Ajdari, and Prost [7] studied rigidly coupled flashing ratchets, where each particle experiences asymmetric interaction force on and off (at intervals). On the other hand, Csahók, Family, and Vicsek [8] investigated a coupled rocking ratchet model, where not only the spatially asymmetric force but also time-periodic external force is applied to the system. The authors have been studying energy efficiency of elastically coupled flashing ratchet models [9,10].

The ratchet models, which are other types of models totally distinct from those in Refs. [11–13], have been studied also as models for molecular motors. Among the molecular motors, acto-myosin motors are widely investigated for muscle contraction, where two kinds of filaments, consisting mainly of actin and myosin (protein) molecules, respectively, play an important role [14,15]. It is considered that they slide past each other using energy of ATP (adenosine triphosphate) hydrolysis and muscle contraction results on a macroscopic scale. If in the flashing ratchet models the particles are re-

garded as heads of actin molecules, the spatially asymmetric interaction force as that between actin and myosin molecules and the on-and-off turning of the asymmetric interaction force as association and dissociation between actin and myosin molecules with the use of energy of ATP hydrolysis, the flashing ratchet models can be investigated as models for acto-myosin motors. In actual muscle contraction, however, the actin molecules do not work independently but move correlatively with neighboring ones, therefore, it is natural to take into account mutual elastic interaction among particles in the ratchet models as more realistic ones for the acto-myosin motors for muscle contraction. Some workers including the present authors investigated the coupled ratchet models as those for muscle contraction [7,9,10].

All the studies referred above on Brownian motors have been done in a one-dimensional space, that is, ratchet models with the particles moving only in a one-dimensional direction are investigated. Recently several authors have investigated characteristics of molecular motors in a two-dimensional space [10,16–24]. Characteristic two-dimensional motion of a ratchet particle was investigated in Refs. [16–18] and rectification and negative mobility were observed for a two-dimensional ratchet model in Ref. [19]. Separation of particles with the use of two-dimensional ratchetlike mechanism was also investigated in Ref. [20]. In Refs. [22,23], two-dimensional Brownian motion is investigated under the influence of a two-dimensional ratchet potential and the motion orthogonal to the applied force is observed. Two-dimensional devices separating two kinds of particles by ratchet mechanism are theoretically investigated in Ref. [24]. We studied a coupled two-dimensional flashing ratchet model and obtained preliminary results [10].

The one-dimensional models are reasonable as those for the molecular motors in muscle contraction because a filament moves on a line in muscle contraction. It is, however, interesting to consider two-dimensional motion of Brownian particles and investigate the dimensional effects on the dy-

namical properties of the model from theoretical points of view. Moreover, in order to explain the results of *in vitro* biological experiments on two-dimensional motion of actin filaments in motility assays [25–27], we must devise two-dimensional Brownian motor models. In this paper, therefore, we extend the elastically coupled ratchet model in a one-dimensional space to that in a two-dimensional space in order to apply it to the experiments.

The biological experiments are as follows [25–27]. A cover glass is coated with myosin molecules, and actin filaments are set on them. When ATP is added in this system and an appropriate environmental condition is set, the actin filaments start to move steadily in their own easily advancing direction in the two-dimensional plane on the cover glass because they interact with the myosin proteins with the use of energy produced by ATP hydrolysis.

In order to construct a model to explain these experiments mentioned above, we have to approximate two points for myosin. First, for simplicity, the characteristic directions of myosin molecules are neglected because the directions of the molecules are distributed randomly in motility assays and in average sense we can treat the molecules as nondirectional ones for a first approximation, although myosin molecules have their own directions to which actin filaments easily advance. Second, also for simplicity, myosin molecules are assumed to be located at two-dimensional square lattice points, and the stable force free points of the interaction force between myosin and actin molecules are set to be the lattice points, although the configuration of the molecules is not entirely periodic. Moreover, extending our coupled model from the one-dimensional one to the two-dimensional one, we must include two characteristics for actin filaments. One is lateral elasticity of the interaction between neighboring particles, which tends for particles to align straight. The other is the characteristic direction, or easily advancing one, of each particle (actin molecule). In our model, each particle has its own easily advancing direction, with which the spatially asymmetric direction of the interaction force is made coincident. The easily advancing direction of each particle is determined to be the approximate tangential direction of the chain, the particles coupled with springs, which corresponds to an actin filament.

It is reported that actin filaments in motility assays advance zig-zag, swaying its body just like a snake. We reproduce such characteristic motion of the particles with computer simulation of our model. Moreover, the motion of the actin filaments shows some interesting aspects in the experiments. Among them, in the present paper, we pay special attention to two points. One is that the longer the actin filament becomes, the smaller the variance of the distribution of the advancing direction becomes in the experiments [26]. We try to reproduce qualitatively the distribution of the change of their advancing direction in our model. The other is the dependence of amplitude of velocity of filaments on density of myosin molecules in motility assays. That is, with increase of the density of myosin molecules, the amplitude of the velocity increases and is saturated for high densities. We investigate the dependence of the amplitude of the velocity on the spatial period (lattice constant) of the stable force free points of the spatially asymmetric interaction force, which is

considered to be inversely proportional to the density of myosin molecules in our model because the higher the density of myosin becomes, the larger the number of the stable force free points, which correspond to the position of the myosin molecule, becomes in a unit area, that is, the shorter the lattice constant of the stable force free points of the interaction force between myosin and actin molecules becomes.

In Sec. II, we explain our two-dimensional Brownian motor model and our simulation results are discussed in Sec. III. We summarize our conclusion in Sec. IV.

II. COUPLED TWO-DIMENSIONAL MODEL

In this paper, our model is described by dimensionless quantities. We consider a chain consisting of N particles which move in a two-dimensional space and are mutually connected with linear elastic springs. The ith particle is denoted by P_i, whose position vector is represented as $\boldsymbol{x}_i = (x_i, y_i)(i=1,\ldots,N)$. The particles experience elastic interaction force, spatially asymmetric interaction force, and random force. The detailed explanations of the respective force are given as follows.

A. Elastic interaction between particles

The particles are elastically coupled with the nearest neighboring ones (see Fig. 1). First, we consider the longitudinal linear elastic interaction between the two nearest neighboring particles, that is, the longitudinal elastic force exerted on the ith particle P_i, by the neighboring $(i+1)$th particle P_{i+1}, $\boldsymbol{f}_{i,i+1}^{\mathrm{LO}}$, is given by

$$\boldsymbol{f}_{i,i+1}^{\mathrm{LO}} = k\left[\sqrt{(\boldsymbol{x}_i - \boldsymbol{x}_{i+1})^2} - a\right]\frac{\boldsymbol{x}_{i+1} - \boldsymbol{x}_i}{\sqrt{(\boldsymbol{x}_i - \boldsymbol{x}_{i+1})^2}}, \quad (1)$$

where k denotes the longitudinal spring constant and a the natural length of the springs. Since the ith particle P_i interacts elastically with two neighboring particles, $(i-1)$th and $(i+1)$th particles, P_{i-1} and P_{i+1}, the interaction force exerted on the ith particle, P_i, for this longitudinal elasticity, $\boldsymbol{F}_i^{\mathrm{LO}}$, is $\boldsymbol{F}_i^{\mathrm{LO}} = \boldsymbol{f}_{i,i+1}^{\mathrm{LO}} - \boldsymbol{f}_{i-1,i}^{\mathrm{LO}}$ (for $i \neq 1, N$). Because we employ free boundary conditions in our model, the longitudinal elastic force for the boundary particles, P_1 and P_N, are given by $\boldsymbol{F}_1^{\mathrm{LO}} = \boldsymbol{f}_{1,2}^{\mathrm{LO}}$ and $\boldsymbol{F}_N^{\mathrm{LO}} = -\boldsymbol{f}_{N-1,N}^{\mathrm{LO}}$, respectively.

Next, we introduce the lateral elasticity exerted on the particles. Without this, particles move easily even in the normal direction of the chain, consisting of the particles coupled with the springs, are apt to be mutually crossed and the chain tends to be heavily folded, which is not favorable characteristics in reproduction of the experimental results as a model for the *in vitro* biological experiments in motility assays, where the filament consisting of actin moves steadily in a certain direction on a two-dimensional plane. To avoid the folding, we introduce elasticity not only in the longitudinal direction already taken into account but also in the lateral direction of our model, which makes the particles tend to align straight (Fig. 1). If we define $\boldsymbol{d}_i$ as $\overrightarrow{H_iP_i}$, where H_i is the foot of the perpendicular from P_i to the line segment $\overline{P_{i-1}P_{i+1}}$,
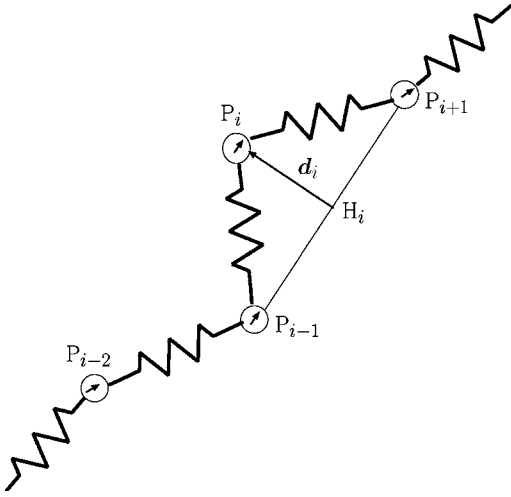
FIG. 1. Schematic illustration of our model. We introduce longitudinal and lateral elasticity. The lateral elastic force exerted on the ith particle P_i ($1 < i < N$) is $-Ad_i$, where A denotes the lateral elastic constant and $d_i = \overrightarrow{H_iP_i}$, where H_i is the foot of the perpendicular from P_i to the line segment $\overline{P_{i-1}P_{i+1}}$. The force is exerted in the direction as the three particles, P_{i-1}, P_i, and P_{i+1}, align straight and therefore folding of the chain consisting of the coupled particles is avoided. The lateral elastic force is not exerted on the two boundary particles, P_1 and P_N. Moreover, each particle has its own easily advancing direction. The direction of each particle (represented by a small arrow on each one) is defined as the average of the direction of the neighboring two springs, in other words, the direction of the line segment, $\overline{P_{i-1}P_{i+1}}$, which links the neighboring two particles. That is, we choose the direction from the $(i-1)$th particle P_{i-1} to the $(i+1)$th particle P_{i+1} as the easily advancing direction of the ith particle P_i.

we set the lateral elastic force exerted on the ith particle, F_i^{LA}, to be equal to $-Ad_i$, where $A(>0)$ stands for the lateral elastic constant, and the minus sign of F_i^{LA} is chosen as the three particles, P_{i-1}, P_i, and P_{i+1}, tend to align straight by the lateral elasticity. The two boundary particles (P_1 and P_N) do not experience such lateral elastic force because of the free boundary conditions.

B. Spatially asymmetric interaction force with flashing

Each particle also experiences the spatially asymmetric interaction force on and off, or occasionally. The flashing (occasional) interaction force exerted on the ith particle, F_i^A, is given by $h_i(t)f_i^A(x_i)$ ($i = 1, 2, \ldots, N$), where $h_i(t)$ represents on-and-off properties of the force and $f_i^A(x_i)$ denotes spatially asymmetric part of F_i^A.

First, $h_i(t)$ is defined as a colored random modulation that rules the time dependent change expected 0 or 1. We choose $h_i(t)$ as follows. Mutually independent Ornstein-Uhlenbeck process $Z_i(t)$ (for $i = 1, \ldots, N$), that is,

$$\langle Z_i(t)Z_j(s)\rangle = \delta_{ij}\frac{D'}{\tau}e^{-|t-s|/\tau}, \tag{2}$$

is considered where the Kronecker's delta $\delta_{ij} = 0$ for $i \neq j$ and 1 for $i = j$, $\langle Z_i(t)\rangle = 0$, $D' = 0.4$, $\langle \cdots \rangle$ means ensemble average

and τ the correlation time. If $Z_i(t)$ is less than 0 then $h_i(t)$ is defined to be 0, and if $Z_i(t)$ is more than or equal to 0 then $h_i(t)$ is set to be 1. Therefore, the particle P_i does not experience the asymmetric force if $h_i(t)$ is equal to 0 and does experience the asymmetric force if $h_i(t)$ is equal to 1. Since the correlation time of $h_i(t)$ is τ, F_i^A, the asymmetric interaction force exerted on the particle, changes stochastically between 0 and $f_i^A(x_i)$ with the correlation time τ, that is, $h_i(t)$ causes the flashing. Since only the sign of $Z_i(t)$ is taken into account, the value of D' is irrelevant to the results.

Next, we explain $f_i^A(x_i)$, the spatially asymmetric part, whose asymmetric direction is set to be the easily advancing direction of the ith particle P_i. The direction of each particle is determined to be roughly the tangential direction of the chain consisting of the particles (see Fig. 1). That is, the easily advancing direction of the ith particle is decided to be that of the line segment, $\overline{P_{i-1}P_{i+1}}$ which links the two neighboring particles, the $(i-1)$th and the $(i+1)$th particles. From two opposite directions of this line segment, we choose the direction from the $(i-1)$th particle to the $(i+1)$th particle as the direction of the particle. Since the two particles, P_1 and P_N, located at the end of the chain have only a single neighboring particle, we define their easily advancing directions as those of the lines which link themselves to the neighboring one, that is, $\overrightarrow{P_1P_2}$ for the first particle and $\overrightarrow{P_{N-1}P_N}$ for the last Nth particle. By this rule, we can assign a "natural" direction to each particle, since roughly speaking, the direction of each particle defined above is approximately the direction of the tangential line of the chain, which, as a model for actomyosin molecular motors, is thought to be approximately coincident with the asymmetric direction in which the actin filament moves easily.

The actual functional form of $f_i^A(x_i)$ is determined as follows. We set the stable force free points of the asymmetric interaction force to be the square lattice points, $x_{mn} = (2bm, 2bn)$ (for $m, n = 0, \pm 1, \pm 2, \ldots$), where $2b$ means the lattice constant of the stable force free points. First, we consider the easiest case. That is, if the easily advancing direction of the ith particle is the positive direction of the x axis, $f_i^{0A}(x_i) = (f_{i,x}^{0A}(x_i), f_{i,y}^{0A}(x_i))$ is chosen as the asymmetric part, $f_i^A(x_i)$, where

$$f_{i,x}^{0A}(x_i) = -U\left[\cos\left(\frac{\pi(x_i + x_0)}{b}\right) + \frac{1}{2}\cos\left(\frac{2\pi(x_i + x_0)}{b}\right)\right], \tag{3}$$

$$f_{i,y}^{0A}(x_i) = -U\sin\left(\frac{\pi y_i}{b}\right), \tag{4}$$

which is asymmetry in the direction of the x axis. U represents the amplitude and $x_0 = -b/\pi \cos^{-1}(-1/2 + \sqrt{3}/2)$. In this case, the stable force free points of Eqs. (3) and (4) are $\{x_{mn}\}$ and the easily advancing direction of P_i by ratchet mechanism is the positive direction of the x axis. Since ordinarily the direction of the ith particle P_i is not coincident with the x axis, for determination of $f_i^A(x_i)$, the above force vector, Eqs. (3) and (4), should be rotated as the direction of asymmetry is set to be the exact easily advancing direction of the ith

particle. For simplicity, we set the nearest stable force free point from the particle, $x_{i,0}$, that is, one of the lattice points $\{x_{mn}\}$, where the amplitude of the asymmetric force is 0, as the axes of the rotation of the asymmetric interaction force. With the use of $\tilde{x}_i$ defined by

$$\tilde{x}_i = x_{i,0} + \begin{pmatrix} \cos\theta_i & \sin\theta_i \\ -\sin\theta_i & \cos\theta_i \end{pmatrix}(x_i - x_{i,0}), \qquad (5)$$

where θ_i stands for the angle between the positive part of the x axis and characteristic direction of the ith particle, $f_i^A(x_i)$ is given by

$$f_i^A(x_i) = \begin{pmatrix} \cos\theta_i & -\sin\theta_i \\ \sin\theta_i & \cos\theta_i \end{pmatrix} f_i^{0A}(\tilde{x}_i). \qquad (6)$$

In this case, although the stable force free points of f_i^A is not generally coincident with $\{x_{mn}\}$ except for $x_{i,0}$, we only use its one-period region near $x_{i,0}$. Therefore, it is no problem for a first approximation.

Although we do not show the results in this paper, we obtain qualitatively similar results when we set the axes of the rotation for determining the asymmetric force to be the position of the particle itself, which is not a reasonable choice [10]. One may think that we should also consider the direction of the myosin head as a model for experiments in motility assays. As explained in Sec. I, we do not, however, take it into account in our model for simplicity, because directions of myosin molecules coated on a cover glass are located randomly on it and there are no characteristic directions on the average sense.

C. Equations of motion

With the use of the force exerted on each particle explained above, the equations of motion for the Brownian particles in our model are as follows ($i = 1, \ldots, N$):

$$\gamma\frac{dx_i}{dt} = F_i^{LO} + F_i^{LA} + F_i^A + F_i^R(t), \qquad (7)$$

where we consider the overdamped case for a friction constant γ. $F_i^R(t) = (\xi_i(t), \eta_i(t))$ (for $i = 1, \ldots, N$) is random force, where $\xi_i(t)$ and $\eta_i(t)$ denote mutually independent white noises of zero mean and correlations $\langle\xi_i(t)\xi_j(s)\rangle = 2\gamma D\delta_{ij}\delta(t-s)$, $\langle\eta_i(t)\eta_j(s)\rangle = 2\gamma D\delta_{ij}\delta(t-s)$, and $\langle\xi_i(t)\eta_j(s)\rangle = 0$ ($i,j = 1, \ldots, N$), where D stands for the temperature, $\delta(t)$ the Dirac's delta function and δ_{ij} the Kronecker's delta.

III. NUMERICAL SIMULATION

We numerically solve the equations of motion (7) by the Euler-Maruyama difference scheme for time mesh $\Delta = 0.0001$. It is confirmed in our simulation that the value of Δ is sufficiently small. At the beginning of our simulations, the ith particle is always located at $(x,y) = (i,0)$. In our simulation, a, τ, and γ are (with nondimensional units) set to be 1.0, k to be 4.0, D to be 0.2, and b to be 2 except in Sec. III C. $a = 1$ and $\gamma = 1$ are chosen as the scales of length and time are determined from them, and $k = 4$ is chosen because
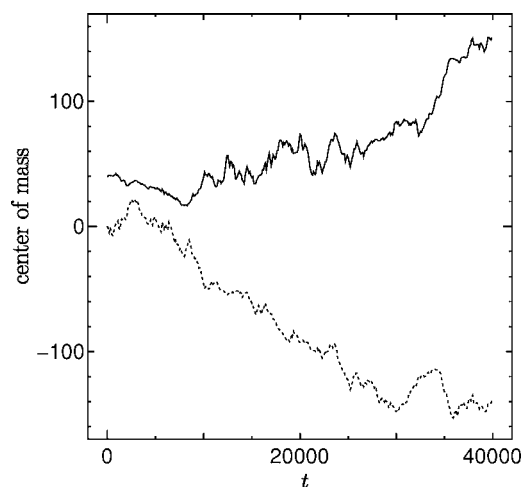

FIG. 2. The center of mass of particles is depicted as a function of time t, where the full line represents the x component and dashed line the y component of the center of mass. From this figure, we know that the particles almost steadily move in a certain direction except for the very early time of the simulation. We set $A = 34$, $U = 1$, and $N = 80$.

in the one-dimensional model the velocity has a maximum for it. Thereby we usually change only three parameters in our simulation, that is, A, U, and N. Only in Sec. III C, we also change the value of b.

A. Motion of particles

For small N, the velocity of the chain increases as a function of N and is saturated approximately above $N = 60$. In Fig. 2, for example, the x and y components of the center of mass of particles are plotted as a function of time t for $A = 34$, $U = 1$, and $N = 80$. Since the values of the x component of the center of mass are almost steadily increasing (the full line) and the y component decreasing (the dashed line) in Fig. 2, the chain consisting of the particles is advancing in a certain direction except for the very early time of the simulation. For other values of parameters, the particles also similarly move steadily in a certain direction. This corresponds to the steady motion of filaments in motility assays. The reason why the advancing direction of the chain is not always coincident with the initial easily advancing direction (the x axis) is that once the tangential direction of the chain becomes inclined to the x axis, the chain moves to its tangential direction and the moving direction of the chain is changed for each simulation result. In Fig. 2, the chain moves to the direction between the positive part of the x axis and negative part of the y axis.

In Fig. 3, three snapshots of the particles for three successive time points are depicted for an example. From this figure, we see that although the particles are moving zig-zag, they steadily advance in a certain direction, which is approximately coincident with the tangential direction of the chain and that we can reproduce the observed results of the experiments in motility assays qualitatively [26]. For other values of parameters, the similar results are obtained, although, for small A, the chain is apt to be folded mutually and the velocity is reduced by it.
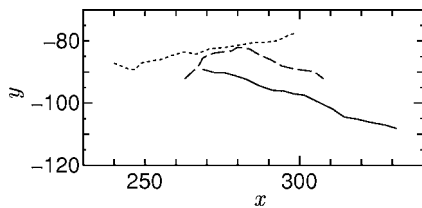
FIG. 3. The dotted line represents a snapshot of the configuration of particles for $t=18\,700$, the dashed line that for $t=20\,000$, and the full line that for $t=21\,500$, where we set $A=34$, $U=3$, and $N=80$. This figure shows that the chain advances zig-zag and moves steadily in the direction which coincides approximately with the tangential one of the chain.

B. Distribution of advancing direction of particles

We investigate the distribution of the angle between the velocity vectors of the center of mass of the coupled particles at two different time points. This angle $\theta(0° \leqslant \theta \leqslant 180°)$ is defined as follows:

$$\theta = \arccos \left| \frac{\boldsymbol{v}(t+T) \cdot \boldsymbol{v}(t)}{v(t+T)v(t)} \right|, \tag{8}$$

where T denotes the time difference between the two time points when the velocity is evaluated. In our simulation, T is set to be 200. We calculate the velocity vector of the coupled particles at time s, $\boldsymbol{v}(s)$, by measuring the difference of the coordinates of the center of mass of the particles, $X(s)$,

$$X(s) = \frac{1}{N}\sum_{i=1}^{N} \boldsymbol{x}_i(s), \tag{9}$$

between s and $s+T_1$ and $\boldsymbol{v}(s)$ is defined as

$$\boldsymbol{v}(s) = \frac{X(s+T_1) - X(s)}{T_1}, \tag{10}$$

and its amplitude is denoted by $v(s)$. In our simulation, T_1 is set to be equal to T. The results are similar to those for $T_1 = 100$.

Figure 4 shows the distribution of θ for $N=20$ and 80, respectively. For $N=20$, the distribution of angle spreads in a wide region of the angle. For $N=80$ case, the distribution concentrates near $\theta=0$ and the wide changes of the advancing direction of the particles become rare events. The longer the chain becomes, the more clearly the distribution concentrates near the angle 0. That is, for the system with a large number of the particles, they move steadily in the almost same direction. Those results are coincident with those of the biological experiments quite well [26]. This fact is another explanation for the results of the N dependence of the velocity of the chain stated in Sec. III A, that is, the velocity of the chain becomes large with increase of N and is saturated for sufficiently large N.

C. The dependence of the amplitude of the velocity of particles on the lattice constant of the stable force free points of the asymmetric interaction force

Finally we investigate the amplitude of the velocity as a function of the spatial period (lattice constant) of the stable
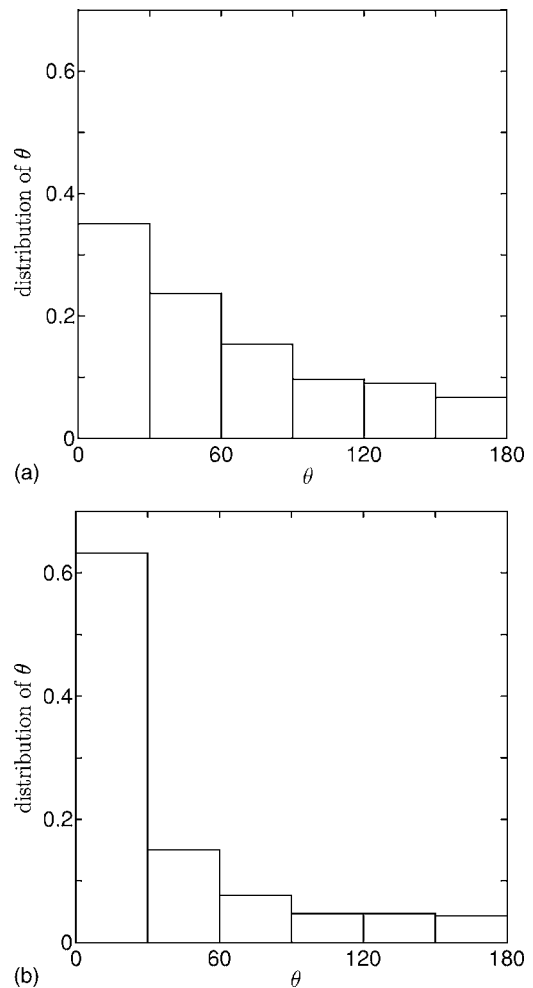

FIG. 4. The angle distribution of the advancing directions of particles for $A=14$ and $U=1$. In the upper figure, the results for $N=20$ and in the lower figure, those for $N=80$ are depicted. For large N, the distribution concentrates near $\theta=0$.

force free points of the spatially asymmetric interaction force, $2b$. From Fig. 5, we see that the amplitude of the velocity of the center of mass increases as a function of the inverse of the period (lattice constant) of the asymmetric force, $1/2b$, and is saturated for large $1/2b$. The amplitude of the velocity for $A=34$ is larger than that for $A=14$. As a function of the lateral elastic constant, A, the amplitude of the velocity also increases and is saturated approximately above 25. Biological experiments in motility assays show the relation between the density of myosin molecules spread all over a cover glass and the amplitude of the velocity of actin filaments interacting with the myosin molecules [27]. The experimental results are as follows. If the density of myosin molecules coated on the cover glass is increased, the amplitude of the velocity of the actin filaments becomes larger in some degree and is saturated for high densities. We investigate this result by changing b of our model in our simulation. As the spatial period (lattice constant) of the stable force free points, $2b$, becomes shorter, the larger number of the stable points with the zero asymmetric interaction force, which correspond to the positions of myosin molecules, is expected to exist per a unit area. That is, the case of small b corresponds
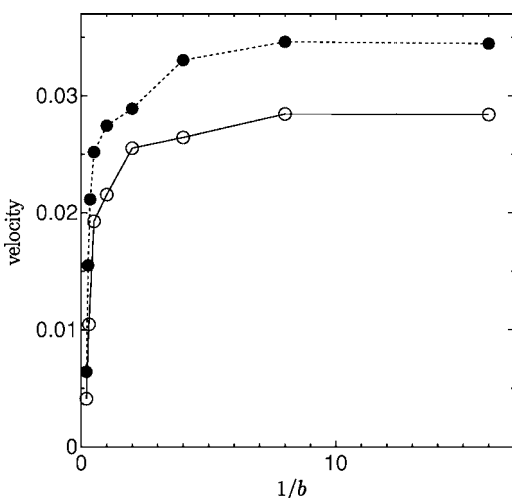
FIG. 5. The $1/b$ dependence of the amplitude of velocity of the center of mass. We set $U=1$ and $N=80$. The open circles and full line represent the results for $A=14$ and the solid circles and dotted line those for $A=34$. The velocity increases with $1/b$ and is saturated for large $1/b$. Those results qualitatively reproduce the experimental results for the dependence of the velocity on the density of myosin molecules.

to the situation with high density of myosin molecules on the cover glass in the biological experiments [27]. From these assumptions, we succeed to reproduce qualitatively the experimental results. Regardless of the elasticity, k and A, of the model, our results show the similar features to those in the biological experiments, that is, increase and saturation of the amplitude of the velocity as a function of $1/b$, or the density of myosin molecules.

Here, we consider the reason for the $1/b$ dependence (increase and saturation) of the amplitude of the velocity. For large b, the distance to a nearest stable force free point is too large and the ratchet mechanism dose not work well because in the time duration τ, which is the average flashing time of the asymmetric interaction force, the chain rarely moves to the next stable force free point of the asymmetric force and the amplitude of the velocity becomes small. Since, with the decrement of b, the ratchet mechanism gradually comes to work, the probability that the particle jumps to the next stable force free point of the asymmetric interaction potential in a flashing time increases and the amplitude of the velocity also increases as a function of $1/b$. For further decreasing of b, however, the efficiency of the ratchet mechanism becomes saturated because the particles almost always jump to the next stable force free points in every flashing occasion and

the average jump distance in a flashing time is mainly limited in the average diffusion distance of the particles during the flashing time. Therefore, for rather small b, the amplitude of the velocity of the chain is saturated since the average advancing distance of the particles in a flashing time depends only on the diffusion distance during τ, but not on b.

IV. CONCLUSION

In this paper, we extend the coupled Brownian motor (ratchet model) from the one-dimensional one into the two-dimensional one and compare the results with the biological experiments.

In order to avoid folding effects of the chain, we introduce not only the longitudinal elasticity but also the lateral elasticity, which forces to align the particles in line. With the lateral elasticity, we succeed to improve our model, that is, steadily advancing motion of unfolded coupled particles is realized. Moreover, we define the easily advancing direction of each particle as the approximate tangential direction of the coupled particles, that is, the direction parallel to the line segment connecting between two neighboring particles and realize the steady motion of the chain consisting of particles in the approximate tangential direction of the chain.

We find some characteristic facts in our two-dimensional extended model. First, we have found that when N is relatively large, the distribution of the change of the advancing direction within a certain time duration concentrates near 0, and the coupled particles move steadily in a particular direction, the tangential one, as shown in Fig. 4. Next, we succeed to reproduce qualitatively the experimental results on the dependence (increase and saturation) of the amplitude of the velocity of actin filaments on the density of myosin molecules from the dependence of the amplitude of the velocity of the chain on $1/2b$, the inverse of the spatial period (lattice constant) of the stable force free points of the asymmetric interaction force.

We have shown that our two-dimensional flashing ratchet model shows quite different features from the one-dimensional ones. Moreover, our improved or naturally extended coupled ratchet model may help to understand mechanism of acto-myosin motors.

[1] R. P. Feynman, R. B. Leighton, and M. Sands, *The Feynman Lectures on Physics* (Addison-Wesley, Reading, 1966), Vol. I, Chap. 46.

[2] R. D. Astumian, Science **276**, 917 (1997) and references cited therein.

[3] P. Reimann, Phys. Rep. **361**, 57 (2002) and references cited therein.

[4] R. D. Astumian and P. Hänggi, Phys. Today **55**(11), 33 (2002) and references cited therein.

[5] P. Reimann and P. Hänggi, Appl. Phys. A: Mater. Sci. Process. **A75**, 169 (2002) and references cited therein.

[6] R. D. Astumian, Philos. Trans. R. Soc. London, Ser. B **355**, 511 (2000).

[7] F. Jülicher, A. Ajdari, and J. Prost, Rev. Mod. Phys. **69**, 1269

(1997) and references cited therein.

[8] Z. Csahók, F. Family, and T. Vicsek, Phys. Rev. E **55**, 5179 (1997).

[9] A. Igarashi, S. Tsukamoto, and H. Goko, Phys. Rev. E **64**, 051908 (2001).

[10] A. Igarashi, H. Goko, and S. Tsukamoto, Physica A **325**, 62 (2003).

[11] A. F. Huxley and R. M. Simmons, Nature (London) **233**, 533 (1971).

[12] H. E. Huxley, Science **164**, 1356 (1969).

[13] T. Duke, Philos. Trans. R. Soc. London, Ser. B **355**, 529 (2000).

[14] T. Yanagida, S. Esaki, A. Hikikoshi Iwane, Y. Inoue, A. Ishijima, K. Kitamura, H. Tanaka, and M. Tokunaga, Philos. Trans. R. Soc. London, Ser. B **355**, 441 (2000).

[15] L. Stryer, *Biochemistry*, 4th ed. (W. H. Freeman, New York, 1995), Chap. 15.

[16] J. Bao and Y. Zhuo, Phys. Lett. A **239**, 228 (1998).

[17] C. Reichhardt and C. J. Olson Reichhardt, Phys. Rev. E **68**, 046102 (2003); C. Reichhardt, C. J. Olson Reichhardt, and M. B. Hastings, *ibid.* **69**, 056115 (2004).

[18] R. Guantes and S. Miret-Artés, Phys. Rev. E **67**, 046212 (2003).

[19] R. Eichhorn, P. Reimann, and P. Hänggi, Phys. Rev. Lett. **88**, 190601 (2002); R. Eichhorn, P. Reimann, and P. Hänggi, Phys. Rev. E **66**, 066132 (2002).

[20] I. Derényi and R. D. Astumian, Phys. Rev. E **58**, 7781 (1998).

[21] C. Keller, F. Marquardt, and C. Bruder, Phys. Rev. E **65**, 041927 (2002).

[22] M. Kostur and L. Schimansky-Geier, Phys. Lett. A **265**, 337 (2000).

[23] M. Kostur, Int. J. Mod. Phys. C **13**, 1157 (2002).

[24] M. Bier, M. Kostur, I. Derényi, and R. D. Astumian, Phys. Rev. E **61**, 7184 (2000).

[25] S. J. Kron and J. A. Spudich, Proc. Natl. Acad. Sci. U.S.A. **83**, 6272 (1986).

[26] Y. Shikata, A. Shikata, R. Shimo, H. Takada, C. Kato, M. Ito, T. Oda, and K. Mihashi, Proc. Jpn. Acad., Ser. B: Phys. Biol. Sci. **70**, 117 (1994).

[27] T. Q. P. Uyeda, S. J. Kron, and J. A. Spudich, J. Mol. Biol. **214**, 699 (1990).